

Biogas to Liquefied Biomethane via Cryogenic Upgrading Technologies

*^aDipartimento di Chimica, Materiali e Ingegneria Chimica “Giulio Natta”, Politecnico di Milano -
Piazza Leonardo da Vinci, I-20133, Italy*

Laura Annamaria Pellegrini^a, Giorgia De Guido^{a,*}, Stefano Langé^a

Email addresses: laura.pellegrini@polimi.it, giorgia.deguido@polimi.it, stefano.lange@polimi.it

*Corresponding author: Giorgia De Guido

Tel.: +39 02 2399 3260

E-mail address: giorgia.deguido@polimi.it

Full postal address: Dipartimento di Chimica, Materiali e Ingegneria Chimica “G. Natta”, Politecnico di
Milano, Piazza Leonardo da Vinci 32, I-20133, Milano, Italy

Abstract

Liquid biomethane (LBM), also referred to as liquid biogas (LBG), is a promising biofuel for transport that can be obtained from upgrading and liquefaction of biogas. With respect to fossil fuels, LBM is a renewable resource, it can be produced almost everywhere, and it is a carbon neutral fuel. LBM is 3 times more energy dense than compressed biomethane (CBM) and it allows longer vehicle autonomy. LBM has also a higher energy density than other transport biofuels, it is produced from wastes and recycled material without being in competition with food production, and it assures a high final energy/primary energy ratio. The low temperatures at which LBM is obtained strongly suggest the use of cryogenic/low-temperature technologies also for biogas upgrading. In this respect, since biogas can be considered as a “particular” natural gas with a high CO₂ content, the results available in the literature on natural gas purification can be taken into account, which prove that cryogenic/low-temperature technologies and, in particular, low-temperature distillation are less energy consuming when compared with traditional technologies, such as amine washing, for CO₂ removal from natural gas streams at high CO₂ content. Low-temperature purification processes allow the direct production of a biomethane stream at high purity

31 and at low temperature, suitable conditions for the direct synergistic integration with biogas
32 cryogenic liquefaction processes, while CO₂ is obtained in liquid phase and under pressure. In this
33 way, it can be easily pumped for transportation, avoiding significant compression costs as for
34 classical CO₂ capture units (where carbon dioxide is discharged in gas phase and at atmospheric
35 pressure).

36 In this paper, three natural gas low-temperature purification technologies have been modelled and
37 their performances have been evaluated through an energy consumption analysis and a comparison
38 with the amine washing process in terms of the equivalent amount of methane required for the
39 upgrading, proving the profitability of cryogenic/low-temperature technologies. Specifically, the
40 Ryan-Holmes, the dual pressure low-temperature distillation process and the anti-sublimation
41 process have been considered. It has been found that the dual pressure low-temperature distillation
42 scheme reaches the highest thermodynamic performances, resulting in the lowest equivalent
43 methane requirement with respect to the other configurations.

44
45 **Keywords:** *biogas upgrading, biomethane, low-temperature, distillation, MEA, energy saving*

46 47 **Nomenclature**

48 *Abbreviations*

| | |
|------------|---------------------------------|
| <i>AHE</i> | Anti-sublimation Heat Exchanger |
| <i>CBM</i> | Compressed Biomethane |
| <i>COP</i> | Coefficient of Performance |
| <i>EU</i> | European Union |
| <i>HP</i> | High Pressure |
| <i>LBG</i> | Liquefied Biogas |
| <i>LBM</i> | Liquefied Biomethane |
| <i>LHV</i> | Lower Heating Value |
| <i>LL</i> | Lean Loading |
| <i>LNG</i> | Liquefied Natural Gas |
| <i>LP</i> | Low Pressure |
| <i>MEA</i> | MonoEthanol Amine |
| <i>ppm</i> | Parts per million |
| <i>PSA</i> | Pressure Swing Adsorption |

RHE Recovery Heat Exchanger

RL Rich Loading

49

50 *Symbols*

\dot{m} Mass flow rate, [kg/s]

K Proportionality constant in Eq. (4), [kg/m³]

n Number of compression stages, [-]

\dot{n} Molar flow rate, [kmol/s]

n-C₄ n-butane

P Pressure, [bar]

\dot{Q} Power, [kW]

T Temperature, [°C]

T_{dew} Dew-point temperature, [°C]

T_0 Ambient temperature, [°C]

\dot{V} Volumetric flow rate, [m³/s]

51

52 *Subscripts*

CH₄ Referred to methane

CO₂ Referred to carbon dioxide

f Referred to the real refrigeration cycle

f,id Referred to the theoretical ideal refrigeration cycle

i Referred to the *i*-th component

S Referred to the solvent

STM Referred to low-pressure steam

MEA Referred to MEA

53

54 *Superscripts*

ABS Absorbed

IN Referred to inlet conditions

OUT Referred to outlet conditions

SPEC Referred to given specifications

55

56 *Greek symbols*

| | |
|-----------------|--------------------------------------|
| ΔH_{Ev} | Latent heat of vaporization, [kJ/kg] |
| η_B | Boiler efficiency, [-] |
| η_{CC} | Combined cycle efficiency, [-] |
| η_{II} | Second law efficiency, [-] |

57

58 **1. Introduction**

59 Biomethane is methane sourced from renewable biomass. The pre-stage of biomethane is better
60 known as biogas, which is produced by anaerobic digestion of organic material, such as manure,
61 sewage sludge, the organic fractions of household and industry waste, and energy crops [1]. Biogas
62 is also produced during anaerobic fermentation in landfills and is, then, referred to as landfill gas.

63 The worldwide biogas production is unknown, but the production of biogas in the European Union
64 in 2013 accounted for 13.4 million tons of oil equivalent (10% increase compared to 2012), which
65 represented 52.3 TWh of electricity produced and net heat sales to heating district networks of 432
66 megatons of oil equivalent [2].

67 The composition of biogas depends on the organic matter present in the waste and on the type of
68 anaerobic digestion process, which in turn depends on the origin of the residue digested [3]. For
69 instance, biogas obtained from the anaerobic degradation of sewage sludge, livestock manure or
70 agroindustrial biowastes contains 53-70% of CH₄ and 30-47% of CO₂ [4-6] together with other
71 impurities.

72 Biogas can be utilized as a fuel for on-site heat, steam and electricity generation in industry, as a
73 substrate in fuel cells, as a substitute of natural gas for domestic and industrial use prior to injection
74 into natural gas grids and as a vehicle fuel [7-9]. Depending on the end use, different biogas
75 treatment steps are necessary. When it is important to have a high energy gas product, *e.g.* as
76 vehicle fuel or for grid injection, the gas needs to be upgraded, *i.e.* CO₂ must be removed.

77 Upgrading of biogas has gained increased attention due to increasing targets for renewable fuel
78 quotes for vehicles in many countries. As a matter of fact, biofuels serve as a renewable alternative
79 to fossil fuels in the EU transport sector, helping to reduce greenhouse gas emissions and to
80 improve the EU security of supply. By 2020, the EU aims to have 10% of the transport fuel of every
81 EU country come from renewable sources such as biofuels.

82 When the end use of biomethane is as a vehicle fuel, the conversion into liquid biogas (LBG) can be
83 profitable: indeed, LBG is more than 600 times space efficient compared to biogas at atmospheric
84 pressure and around 3 times more space efficient compared to compressed biogas (CBG) at 200 bar.
85 There are two main ways to produce LBG, namely cryogenic/low-temperature upgrading
86 technologies, where the purified gas is obtained directly at low temperatures, and conventional

87 upgrading technologies (water scrubbing, chemical scrubbing, PSA, membranes) [10-12] coupled to
88 a small-scale liquefaction plant. Since biogas can be considered as a particular natural gas with a
89 high CO₂ content, the results already available in the literature on natural gas purification can be
90 taken into account, which suggest that low-temperature processes, and in particular those based on
91 distillation, require less energy than conventional purification technologies, such as amine
92 scrubbing [13].

93 This work compares the performances of three biogas upgrading technologies operated at low
94 temperatures, namely the Ryan-Holmes extractive distillation process [14, 15], a recently developed
95 dual pressure low-temperature distillation process [16] and the anti-sublimation process [17], with
96 those of a conventional purification process, based on the use of a monoethanolamine (MEA)
97 aqueous solution. After the description of these upgrading technologies, the method adopted for
98 performing the energy analysis is outlined. The results of the analysis are then discussed, showing
99 that the use of cryogenic/low-temperature technologies is synergistic with the cryogenic
100 temperature (about -160°C) required for LBG production, resulting in energy savings for the overall
101 process. Another advantage in using cryogenic/low-temperature technologies is that CO₂ is
102 obtained as a clean liquid product that could be used in further applications.

103

104 **2. Description of process solutions**

105 For all the process solutions considered in this work for removing CO₂ from raw biogas, feed and
106 products conditions are the same in order to better perform the comparison on an energy basis. The
107 feed stream is raw biogas at 35°C and 1 atm. The composition is 40 mol% of CO₂ and 60 mol% of
108 CH₄. The final biomethane has been considered as liquid at atmospheric pressure, with a CO₂
109 content below 50 ppm, as recommended for LNG production [18] to avoid freezing problems
110 during liquefaction. In the two low-temperature processes based on distillation (where the purified
111 methane stream is obtained under pressure) the LBM production train has been assumed to consist
112 of a turbine followed by a cooler: the chosen sequence of operations is not intended to represent the
113 best process configuration, but only a reasonable process solution to bring pressure and temperature
114 levels to the LBM storage ones. For the produced CO₂ stream, the mole fraction of CH₄ has been
115 set to 1.0e-4 in order to enhance the methane recovery and to maintain the same standards adopted
116 for the design of the dual pressure low-temperature distillation process [16]. Regarding its final
117 conditions, the goal is to obtain it in liquid phase under pressure (50 bar), which makes it suitable
118 for further uses. No dehydration steps have been considered in any case, neither for low-
119 temperature technologies nor for the MEA scrubbing process, since all of them require to remove
120 water either before or after the upgrading step. Indeed, for the MEA scrubbing process water is

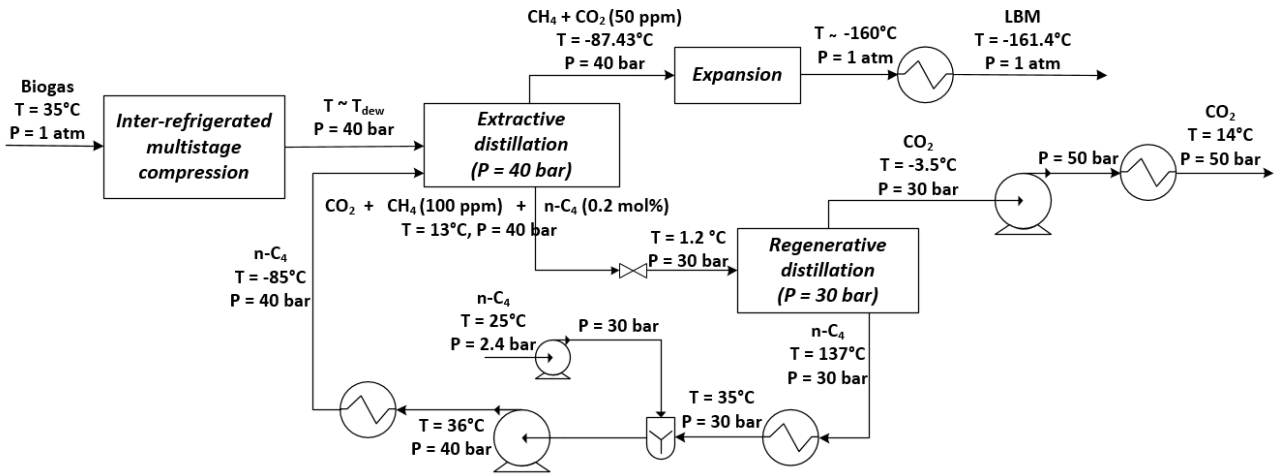
121 removed after the purification section since it is given by saturation conditions at the outlet of the
122 absorber. On the contrary, for the low-temperature distillation processes water is removed before
123 the upgrading step: in this case, the water content of the raw biogas is not known *a-priori* since it is
124 related to previous treatments. Generally, biogas compression will help to remove part of the water
125 by condensation and, thus, a subsequent step to remove water will be needed to reach the final
126 specifications for low-temperature processing. Also in the anti-sublimation process water has to be
127 captured to avoid that water vapor freezes on the low-temperature evaporators, blocking the flue
128 gases passages: this is accomplished at successive levels of temperature, first by condensation and
129 then by a frosting/defrosting process [17].

130 The complete process simulation has been performed only for the low-temperature processes, while
131 for the amine sweetening unit widely used and tested rules of thumb have been employed to
132 estimate the major energy costs related to the purification part. Thus, for the scheme with upgrading
133 by MEA scrubbing only the biomethane and CO₂ liquefaction trains have been simulated. Process
134 simulations have been performed with the commercial process simulator Aspen Hysys[®] [19], using
135 the SRK equation of state [20] that is suitable to represent the phase behavior of the mixture
136 considered in this work, which is commonly found in the gas industry. The number of theoretical
137 stages used for the distillation columns in each process scheme has been chosen in order to take into
138 account a qualitative trade-off between energy consumptions and the total height of the distillation
139 column. The selection of the number of theoretical trays starts from literature case studies [16, 21].

140

141 **2.1 The Ryan-Holmes process**

142 The Ryan-Holmes process [14, 15] performs the removal of carbon dioxide by means of an
143 extractive distillation in order to increase the critical locus of the CH₄-CO₂ system and, at the same
144 time, to move the freezing line to lower temperatures and pressures. Normally, hydrocarbons
145 heavier than methane are used as entrainer and, in particular, n-butane [14, 15, 22]. The process
146 scheme is illustrated in Fig. 1.



148

149 **Fig. 1.** Process Flow Diagram of the Ryan-Holmes process.

150

151 The unit consists of five main parts: the biogas compression section (*Inter-refrigerated multistage*
 152 *compression*), the extractive distillation unit (*Extractive distillation*), the entrainer regeneration
 153 section (*Regenerative distillation*), the biomethane liquefaction train (*Expansion*, followed by the
 154 final heat exchanger) and the CO₂ pump.

155 Since the process is operated under pressure, the inlet biogas feed is compressed from atmospheric
 156 pressure to about 40 bar before entering the extractive distillation section. The demethanizer
 157 column (*Extractive distillation*) is co-fed with n-butane as additive to avoid CO₂ freezing and to
 158 increase the distillation performances. This first distillation column has 40 theoretical trays. The
 159 position of the feed, at the 18th stage from the top, has been chosen in order to minimize the
 160 required duties, while the entrainer is fed on the third tray from the top of the distillation column to
 161 avoid its entrainment in the produced stream. The n-butane flow rate is 10 moles/100 moles of feed
 162 [23]. The entrainer stream (*n-C₄*) conditions have been fixed in order to create the minimum
 163 discontinuity in column profiles: its temperature and pressure levels (-85°C, 40 bar) have been
 164 chosen to be closed to the ones obtained on the third tray of the distillation column (*Extractive*
 165 *distillation*). The *Extractive distillation* top product stream is, then, sent to the liquefaction train, to
 166 obtain the final liquefied biomethane product stream (*LBM*).

167 The bottom product stream from the *Extractive distillation* section contains CO₂ and the entrainer.
 168 This stream is expanded to 30 bar, to remain under the n-butane critical pressure, and it is fed on the
 169 31st stage (from the top) of the *Regenerative distillation* unit (40 theoretical trays), where carbon
 170 dioxide is separated from n-butane. Carbon dioxide is recovered from the top in liquid phase by
 171 means of a total condenser. It is pumped to 50 bar to reach the desired conditions for the CO₂ final

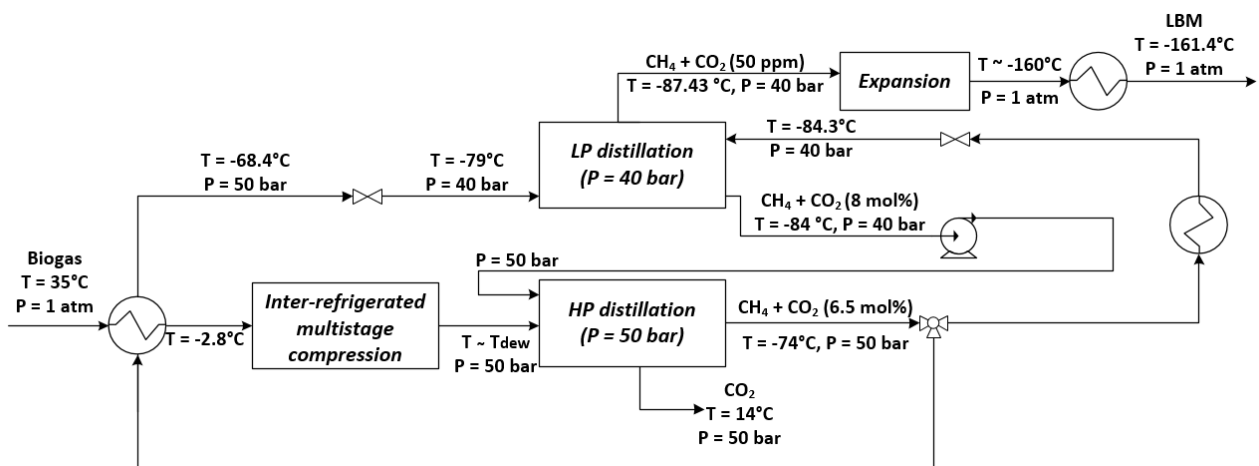
172 stream and, then, it is heated up to 14.06°C (the same temperature as that of the CO₂ obtained from
 173 the dual pressure low-temperature distillation process described in Section 2.2). The bottom stream
 174 from this column contains mainly n-butane, which has to be recycled to the *Extractive distillation*
 175 section. To ensure the conditions required by the process, this stream has to be integrated with an
 176 appropriate make-up stream, pumped and cooled down to the desired conditions. This process is
 177 considered to belong to the class of low-temperature separation processes because of the
 178 temperature profile established in the *Extractive distillation* unit: the temperature decreases from
 179 13.06°C at the bottom reboiler down to -87.3°C at the top condenser. The regeneration column
 180 operates at higher temperature levels: the condenser temperature is close to -3.5°C and the bottom
 181 one is 137°C. Therefore, the energy demand for the extractive distillation is mainly determined by
 182 the condenser duty, while the reboiler duty plays the most significant role for the regeneration
 183 column. The final biomethane is liquefied through the sequence of operation previously outlined,
 184 consisting of a flashing liquid expander [22] followed by a final condenser, that allows to obtain
 185 biomethane in liquid phase and at atmospheric pressure.

186

187 2.2 The dual pressure low-temperature distillation process

188 In the scheme reported in Fig. 2, the upgrading of raw biogas is performed by means of a dual
 189 pressure low-temperature distillation process [16].

190



191

192 **Fig. 2.** Process Flow Diagram of the dual pressure low-temperature distillation process.

193

194 In this process, the purification section consists of two distillation units: the first one is operated at
 195 high pressure (*HP distillation*, 50 bar), above the maximum of the freezing locus of the CO₂-CH₄
 196 system, while the second one at low pressure (*LP distillation*, 40 bar), below the methane critical
 197 pressure. The number of theoretical trays for these two distillation units is 25 and 20, respectively.

198 The HP section can be conceived as the stripping section of a common distillation column: it
199 presents only a reboiler, while the liquid reflux is provided by recycling the liquid stream coming
200 from the bottom of the LP section. In the same way, the LP section works as the enrichment section
201 of a classic distillation column: it has a partial condenser at the top and the gas feed stream is the
202 top product of the HP section. The produced gas stream from the top of the LP section is methane at
203 the required purity specification. Liquid biomethane is, then, produced by means of a proper
204 liquefaction train, which has been assumed to consist of a gas turbine followed by a cooler as for
205 the Ryan-Holmes process. The bottom product from the *HP distillation* section is highly pure
206 carbon dioxide. The biogas feed stream is precooled in a first heat exchanger that uses the available
207 cooling duty of an intermediate process stream, which needs to be heated before being fed to the LP
208 section. The precooled biogas is then compressed to 50 bar and further cooled down to its dew point
209 at 50 bar, before entering the *HP distillation* section. The compression is performed after the
210 precooling of the biogas in order to reduce the compression power by decreasing the temperature of
211 the inlet feed stream. According to the phase behavior of the CO₂-CH₄ mixture [24], no freezing
212 can occur during distillation at about 50 bar. The HP section performs a bulk removal of the inlet
213 CO₂: the bottom stream is liquid CO₂ at high pressure, while the top product stream is a methane-
214 rich gas stream (with about 6.5 mol% of CO₂). Since the HP section operates at a pressure above
215 the methane critical one (*i.e.*, 45.9 bar), it is not possible to obtain pure methane by performing the
216 distillation in a single unit operated at 50 bar. Thus, the final purification is performed in the LP
217 section, operated at 40 bar. The produced streams from the LP section are a top methane gas stream
218 and a bottom methane-rich liquid stream that is pumped back to the HP section. The feed stream
219 enters the HP section on the fourth tray from the top, while the liquid reflux, coming from the
220 bottom of the LP section, is pumped and fed on the first tray from the top. The top gas stream from
221 the HP section is sent to a splitter, which separates it into two streams. Before entering the bottom
222 of the LP section, a part of the HP section top product stream is heated up and expanded to the
223 operating pressure of the LP section, so that it is at a temperature 5-6 K higher than its dew point
224 temperature at the operating pressure of the LP section. This guarantees that no solid phase is
225 formed during the expansion. The heat needed for this operation is taken from the inlet raw biogas
226 stream that is precooled before the compression train. The remaining part of the HP section top
227 product stream is cooled down at 50 bar (away from the CO₂ solubility boundary) and expanded to
228 the operating pressure of the LP section in order to obtain a liquid stream at its bubble point, which
229 is fed to the LP section one theoretical tray above the gas feed stream. The split factor of the HP
230 section top product stream is chosen in order to keep the CO₂ level below 8 mol% in the LP section
231 bottom product stream for avoiding CO₂ freezing. The reflux ratio for the LP distillation has been

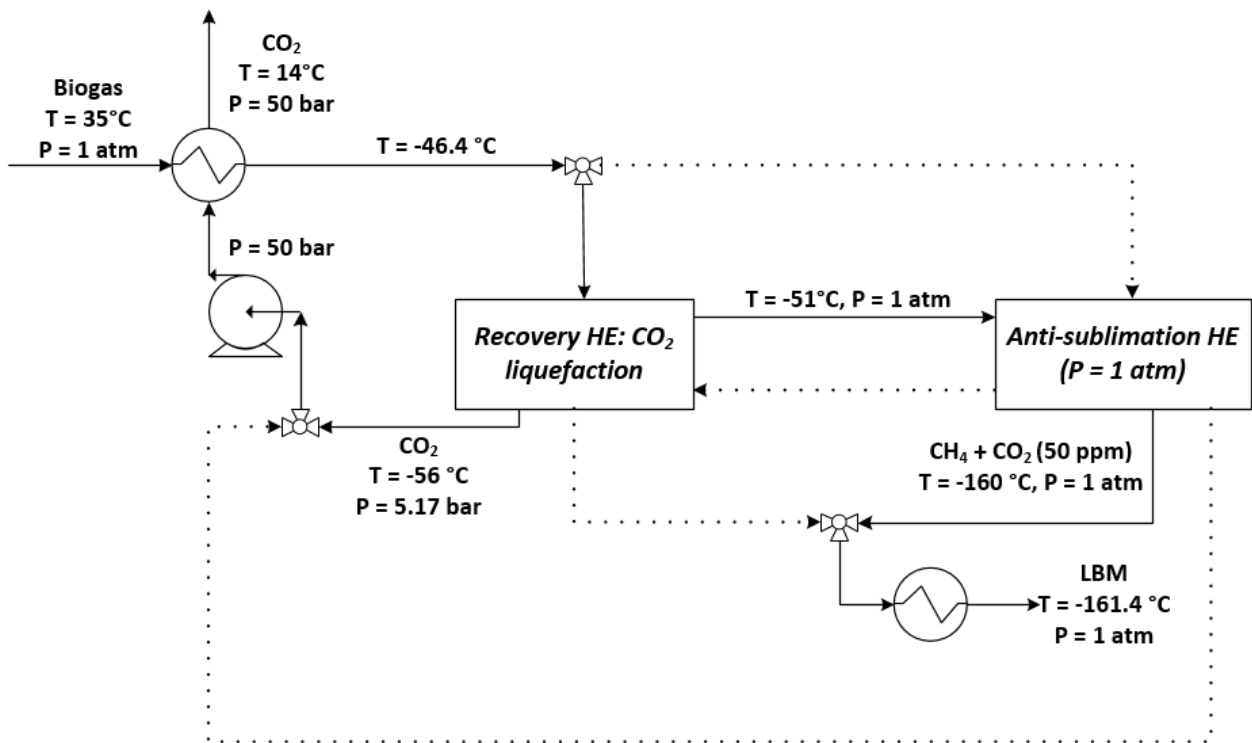
232 set to 2.4.

233

234 2.3 The anti-sublimation process

235 The liquefied biomethane production by means of the anti-sublimation process [25, 26] employs
236 heat exchanger surfaces to upgrade the biogas by operating in the solid-vapor equilibrium region
237 [23] at atmospheric pressure: CO₂ is frosted from the gas stream that is, consequently, enriched in
238 methane. The scheme adopted for this process is shown in Fig. 3.

239



240

241 **Fig. 3.** Process Flow Diagram of the anti-sublimation process.

242

243 In the anti-sublimation process the purification is performed allowing dry ice formation in a closed
244 and dedicated unit operation. In the scheme illustrated in Fig. 3, two heat exchangers are operated in
245 dynamic mode, carrying out the purification (*Anti-sublimation Heat Exchanger*, hereafter denoted
246 by AHE) and the regeneration (*Recovery Heat Exchanger*, hereafter denoted by RHE) phases
247 switching the flow path through these two equipment, ensuring the continuous operation of the
248 process. Different line styles (solid and dotted lines) have been adopted in order to describe the
249 material flows direction according to the working phase alternation: solid lines are used for the
250 operation phase, while dotted lines denote the regeneration one. The raw biogas stream, which is at
251 35°C and at atmospheric pressure, is sent to a heat exchanger, where it is cooled down by means of

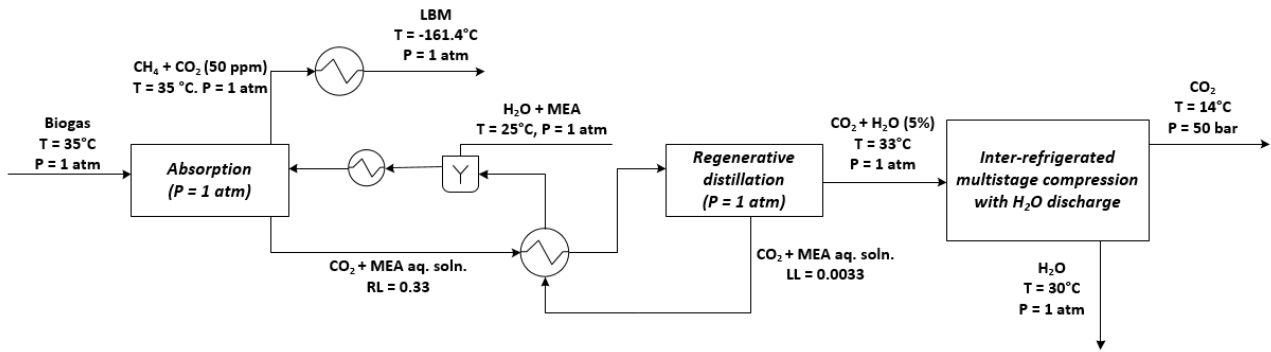
252 cold recovery from the liquefied CO₂ coming from the RHE. The amount of heat recovery is
253 defined in order to warm the liquid CO₂ stream up to 14°C at 50 bar, assuming a minimum
254 temperature approach of about 5 K. The cold biogas is fed to the RHE. The dry ice layer deposited
255 during the previous operating cycle, when the RHE worked as AHE, provides part of the cooling
256 duty to the biogas stream and this allows to reach temperatures down to -51°C by melting the dry
257 ice that is recovered as liquid CO₂ at its triple point. In order to avoid pinch problems, a minimum
258 approach equal to 5 K is kept between the temperatures of the outlet cold biogas and of the liquid
259 CO₂. The liquid CO₂ stream is then pumped to 50 bar and heated in the heat recovery equipment
260 previously described. The cold biogas from the RHE is then fed to the AHE. To achieve CO₂ anti-
261 sublimation a supplementary cooling power is necessary to decrease the temperature (down to -
262 160°C) and frost CO₂ to meet the desired specification on the final product. The cooling duty
263 necessary to perform this operation is supplied by an external refrigeration cycle. Inside the AHE, a
264 solid CO₂ layer grows and a gas stream with 50 ppm of CO₂ is available at atmospheric pressure.
265 The produced gas is then liquefied for the final purpose. A heat exchanger using an external cooling
266 medium is used for this scope. Once the RHE is cleaned and ready to support dry ice formation and
267 the AHE presents a solid CO₂ layer that needs to be liquefied and recovered, a switch between the
268 RHE and the AHE is performed to assure the continuity of the purification and liquefaction
269 operation. Since the formation of a CO₂ solid phase occurs, which is not taken into account in
270 Aspen Hysys[®] [19], the anti-sublimation process has been simulated according to heat and material
271 balances across the RHE and the AHE sections [23].

272

273 **2.4 The chemical absorption process**

274 The fourth considered process solution, illustrated in Fig. 4, is a conventional chemical scrubbing
275 process with an aqueous MEA solution as solvent. For applications at low pressures, such as carbon
276 capture from power plant flue gases, MEA is typically preferred to other amines as chemical
277 solvent, since it shows faster CO₂ absorption kinetics also at low pressure [27].

278



279

280 **Fig. 4.** Process Flow Diagram of the MEA scrubbing process.

281

282 The biogas feed is sent to the absorption column (*Absorption*), where it is contacted
 283 countercurrently with the lean MEA solution. The purified gas stream is obtained at the top of the
 284 absorber and the rich solvent at the bottom, containing the CO₂ to be removed. The rich solvent is
 285 heated in the intermediate cross heat exchanger and sent to the regeneration column (*Regenerative
 286 distillation*), where CO₂ is stripped from the solvent and obtained as gas at the top, while the lean
 287 regenerated solvent is recovered at the bottom of the column. The hot lean stream is cooled in the
 288 intermediate cross heat exchanger and is further cooled before being recycled to the absorber. The
 289 intermediate heat exchanger is used to favour the internal process heat recovery.

290 Make-up of water and amine is needed due to leakages occurring during solvent regeneration. To
 291 reduce the make-up, the regenerator condenser can be operated at the lowest possible temperature
 292 compatible with the available utilities (30°C has been assumed in this work, which is in the range
 293 typically reported in the literature [28], *i.e.* 30-50°C).

294 In this work, a 30 wt% amine aqueous solution has been assumed as solvent.

295 The rich loading (*RL*) has been set to 0.33 (moles of CO₂ per moles of MEA) [27, 29]. The limiting
 296 value of the rich loading is selected considering the lifetime of the plant. The rich solution is highly
 297 corrosive due to the presence of dissociated acidic electrolytes in the aqueous solutions and a
 298 reasonable value is generally fixed from the experience on existing purification units.

299 The lean solvent is regenerated to obtain an acid lean loading (*LL*) equal to 1/100 of the rich loading
 300 [28].

301 Heat to the reboiler of the regeneration column is supplied using low-pressure steam at 3.5 bar. In
 302 the literature, several useful correlations are available [27, 29] to estimate energy consumptions,
 303 particularly regarding process heat supplied to the reboiler of the regeneration column. Compared to
 304 the other studied process solutions, this scheme typically operates at ambient or higher
 305 temperatures. In this way, the most relevant energy consumptions in the amine scrubbing process
 306 are related to the solvent regeneration column. Generally, according to rules of thumb, linear

307 relations between steam consumptions (and, thus, thermal power) and the volumetric flow rate of
 308 the circulating solvent (that takes into account the effect of the inlet CO₂ content of the raw gas) can
 309 be used for the estimation of the reboiler duty. The rule of thumb adopted in this work assumes that
 310 the proportionality constant, K , giving the consumption of LP steam per m³ of lean circulating
 311 solution, is equal to 120 kg/m³ [27, 29].

312 To determine the lean amine flow rate, it is necessary to calculate the amount of the absorbed acid
 313 gas (CO₂) to purify the raw biogas stream to the required specification. Knowing the raw biogas
 314 flow rate and composition, it is possible to compute the molar flow of the absorbed acidic
 315 compound from eq. (1), where $x_{CO_2}^{SPEC}$ is the specification for CO₂ in the purified gas at the absorber
 316 outlet.

$$\dot{n}_{CO_2}^{ABS} = \dot{n}_{CO_2}^{IN} - \frac{\dot{n}_{CH_4}^{OUT} (x_{CO_2}^{SPEC})}{1 - x_{CO_2}^{SPEC}} \quad (1)$$

317 The MEA aqueous solvent flow rate can be so determined knowing the total molar flow of the
 318 absorbed acid gas, the rich loading of 0.33 and the lean loading of 0.0033. In this way, the
 319 difference between the rich and the lean loadings is the ratio between the absorbed CO₂ and the
 320 moles of amine in the solvent. Thus, it is possible to calculate the molar flow rate of MEA in the
 321 aqueous solution (eq. (2)) and, therefore, the molar flow rate of the solvent.

$$\dot{n}_{MEA} = \frac{\dot{n}_{CO_2}^{ABS}}{RL - LL} \quad (2)$$

322 To calculate the steam consumption at the reboiler, it is necessary to determine the volumetric flow
 323 rate of the circulating lean solvent from eq. (3), where the molar concentration (C_{MEA}) of the solvent
 324 (44 kmol/m³ at 30°C and 1 atm) is calculated from the densities of MEA and water.

$$\dot{V}_S = \frac{\dot{n}_S}{C_{MEA}} \quad (3)$$

325 It is, then, possible to determine both steam consumption and the duty at the regeneration column
 326 reboiler, through eq. (4) and eq. (5), respectively.

$$\dot{m}_{STM} = \dot{V}_S \cdot K \quad (4)$$

$$\dot{Q} = \dot{m}_{STM} \cdot \Delta H_{Ev, H_2O}^{3.5bara} \quad (5)$$

327 In eq. (5), $\Delta H_{Ev, H_2O}^{3.5bara}$ is the mass latent heat of vaporization of water at 3.5 bara and its value is 2148
 328 kJ/kg at a boiling temperature of 140°C [30].

329 The liquid biomethane production is performed by direct cooling since the gas is available at
 330 atmospheric pressure, assuming that the dehydration of the produced gas is not taken into account,

331 as previously stated. Since from the top of the regeneration column the CO₂ is obtained wet and at
332 low pressure, to reach the same conditions as in the other schemes some additional treatments are
333 necessary, which include a compression train, condensates separation and final cooling.
334 The inter-refrigerated compression has been designed considering three stages and the outlet
335 pressure from each compression stage has been calculated according to eq. (6), where P_{out}/P_{in} is the
336 global compression ratio between the outlet and inlet pressures of the fluid in the total compression
337 train, n is the number of compression stages and ΔP_{HE} is the pressure drop (set to 0.1 bar) in every
338 intercooler.

$$P_n = P_{n-1} \left(\frac{P_{out}}{P_{in}} \right)^{\frac{1}{n}} + \Delta P_{HE} \quad (6)$$

339 The outlet temperature from intercoolers has been fixed to 30°C.

340

341 **3. Methods**

342 The energy analysis and the comparison of the different proposed process solutions considered for
343 biogas upgrading have been performed by means of the net equivalent methane approach [23] that
344 accounts for the amount of biomethane required by defined reference processes to deliver thermal
345 and mechanical energy to each one of the analyzed processes. The aim is to reduce the involved
346 energy contributions to the same basis, ensuring a coherent assessment of the performances for each
347 process.

348 Heat and mechanical works have been converted into the corresponding amounts of CH₄ required to
349 produce the same duty. In the examined processes, energy is supplied and/or removed at different
350 temperature levels. When low or cryogenic temperatures are required, the cooling duty has been
351 assumed to be produced by a proper refrigeration cycle, while when heat at temperatures around
352 100-150°C is needed, the thermal duty has been considered as low-pressure (LP) steam produced
353 by a CH₄-fired boiler. The heat removed from streams at temperatures higher than 100°C has been
354 assumed equal to the one of an equivalent LP steam potentially available for further uses into the
355 process. The mechanical work produced by turbines or required by compressors and pumps has
356 been considered as electric energy obtained by means of an equivalent CH₄-fired combined cycle
357 power plant.

358 The net energy consumption of each process has been determined, in this way, as the net CH₄
359 requirement. Energy consumptions (refrigeration, heating at high temperatures, compression and
360 pumping) have been assumed as CH₄ consumptions, while energy productions (turbine expansions
361 or heat removed at high temperatures) have been accounted as CH₄ productions.

362 When an energy stream is used to heat a process stream over the ambient temperature, it has been
 363 related to the thermal energy generated by a boiler fed with CH₄ and producing LP steam, according
 364 to eq. (7), where \dot{Q} is the thermal power, η_B is the boiler efficiency, LHV_{CH_4} is the lower heating
 365 value of methane and \dot{m}_{CH_4} is the equivalent flowrate of biomethane required by the boiler.

$$\dot{m}_{CH_4} = \frac{\dot{Q}}{\eta_B \cdot LHV_{CH_4}} \quad (7)$$

366 When cooling at low temperatures is needed, a real refrigeration cycle has been considered. Its
 367 Coefficient of Performance (COP_f) has been calculated starting from the theoretical ideal one
 368 ($COP_{f,id}$), obtained from the Carnot ideal cycle definition [31], corrected by a second law efficiency
 369 defined as the ratio between the actual thermal efficiency and the maximum possible (reversible)
 370 one at the same conditions [32]. It is a measure of how the performances of an actual process
 371 approximate the ones of the corresponding reversible process [33]. In this way, the request of
 372 cooling duty is calculated in terms of the equivalent CH₄ necessary to supply mechanical power to
 373 the refrigeration cycle compressors. This energy has been assumed as electric energy produced by a
 374 CH₄-fired combined cycle power plant. The theoretical ideal COP can be calculated according to
 375 eq. (8), where T_0 is the ambient temperature (25°C) and T is the required low-temperature level.

$$COP_{f,id} = \frac{1}{\frac{T_0}{T} - 1} \quad (8)$$

376 The COP_f of the real refrigeration cycle is given by eq. (9), where η_{II} denotes the second law
 377 efficiency.

$$COP_f = COP_{f,id} \cdot \eta_{II} \quad (9)$$

378 The COP_f also represents the ratio between the provided cooling duty (\dot{Q}_{Cold}) and the electrical
 379 energy consumed (\dot{W}_{EL}) by the cycle (eq. (10)).

$$COP_f = \frac{\dot{Q}_{Cold}}{\dot{W}_{EL}} \quad (10)$$

380 To transform the cooling duty into the equivalent CH₄ consumption, it is necessary to calculate the
 381 mechanical work required by the refrigeration cycle. CH₄ is, then, calculated according to eq. (11),
 382 where η_{CC} is the efficiency of the combined cycle, defined as the ratio between the net power output
 383 and the thermal power input coming from CH₄ combustion.

$$\dot{m}_{CH_4} = \frac{\dot{W}_{EL}}{\eta_{CC} \cdot LHV_{CH_4}} = \frac{\dot{Q}_{Cold}}{COP_f \cdot \eta_{CC} \cdot LHV_{CH_4}} \quad (11)$$

384 The powers related to pumps, turbines and compressors have been calculated (eq. (12)) in terms of
 385 equivalent CH₄ considering the same assumption adopted for the mechanical power in the
 386 refrigeration cycle.

$$\dot{m}_{CH_4} = \frac{\dot{W}_{EL}}{\eta_{CC} \cdot LHV_{CH_4}} \quad (12)$$

387 Table 1 summarizes the values adopted for the lower heating value of methane, the efficiencies of
 388 the combined cycle and of the boiler, the second law efficiency for refrigeration cycles and the
 389 COP_f calculated by eq. (9) for the refrigeration cycles needed to reach the different low
 390 temperatures (as indicated in Table 1) encountered in the processes considered in this work for
 391 comparison purposes.

392

393 **Table 1.** Values of the parameters used to calculate the biomethane equivalent to process energy
 394 streams.

| Parameter | Parameter Value | Reference |
|------------------------|-----------------|-----------|
| LHV_{CH_4} [MJ/kg] | 50 | [34] |
| η_{CC} [-] | 0.55 | [35] |
| η_B [-] | 0.8 | [36] |
| η_{II} [-] | 0.6 | [37] |
| COP_f (@ -165°C) [-] | 0.34 | This Work |
| COP_f (@ -100°C) [-] | 0.83 | This Work |
| COP_f (@ -35°C) [-] | 2.38 | This Work |
| COP_f (@ -10°C) [-] | 4.51 | This Work |

395

396 **4. Results and discussion**

397 The method previously outlined has been applied to the studied process configurations illustrated in
 398 Figs. 1-4 for comparing their relative performances in terms of net equivalent biomethane. In order
 399 to extend and generalize the results, the net equivalent biomethane can be expressed in terms of
 400 percentage of produced biomethane useful to supply energy to the process (eq. (13)).

$$\%_{LBM} = \frac{\dot{m}_{CH_4,consumed} - \dot{m}_{CH_4,produced}}{\dot{m}_{CH_4,raw\ BG}} \quad (13)$$

401 The results of the overall performances of the different processes are reported in Table 2.

402

403

404 **Table 2.** Percentages of the total produced biomethane required by the different investigated
 405 processes for LBM production.

| Process | %<i>LBM</i> |
|--|--------------------|
| Ryan-Holmes | 15.70 |
| Dual pressure low-temperature distillation | 14.00 |
| Anti-sublimation | 21.79 |
| MEA scrubbing | 29.00 |

406
 407 Low-temperature processes require to use a lower amount of the produced biomethane to supply
 408 energy to the process. Among them, the anti-sublimation process is the most energy-intensive, since
 409 the operation is performed by means of a direct phase change (frosting) in a single unit operation,
 410 where the cold utility is at constant temperature. On the contrary, operations based on distillation
 411 (like the Ryan-Holmes and the dual pressure low-temperature distillation processes) are
 412 characterized by a space-distributed energy profile allowing a better use of cold utilities. The
 413 process with the lowest energy consumptions is the dual pressure low-temperature distillation
 414 process, while the Ryan-Holmes process is slightly more energy-intensive. This is due to the heat
 415 required for solvent regeneration that occurs at high temperature (137°C, as shown in Fig. 1).
 416 The contributions to the energy performances of each process can be better analysed in two ways,
 417 considering the energy distribution by quality (mechanical power, cooling and heat duties) and the
 418 energy distribution by operation (biogas compression, upgrading, CO₂ pressurization and
 419 biomethane liquefaction).

420 As for the energy distribution by quality, the results in terms of percentages of the total energy
 421 requirements are reported in Table 3 for each of the investigated processes.

422

423 **Table 3.** Distribution of the energy consumptions by quality.

| Process | Mechanical power consumption [%] | Cooling duties consumption [%] | Heating duties consumption [%] |
|---|---|---|---|
| Ryan-Holmes | 33.55 | 54.37 | 12.07 |
| Dual pressure low- temperature distillation | 38.77 | 61.23 | 0.00 |
| Anti-sublimation | 0.16 | 99.84 | 0.00 |
| MEA scrubbing | 7.78 | 34.82 | 57.40 |

424

425 If the dual pressure low-temperature distillation process is compared with the Ryan-Holmes
 426 process, the former requires the highest mechanical power as a result of the higher pressure the raw
 427 biogas is compressed to (50 vs. 40 bar). Moreover, the dual pressure low-temperature distillation
 428 process also requires the highest cooling duty since it employs two condensers operated at low
 429 temperatures for performing the desired purification, while in the Ryan-Holmes process only one
 430 condenser at low temperature is needed. The disadvantage of the Ryan-Holmes process is the need
 431 of heat (LP steam) for solvent regeneration at about 137°C, which accounts for 12% of the total
 432 energy demand. On the contrary, for the reboiler of the HP section of the dual pressure low-
 433 temperature distillation process water can be used as service fluid to provide heat, since the
 434 temperature level is 15°C. For these two low-temperature processes, the mechanical power that can
 435 be recovered inside the process by means of the expander does not play a significant role: it is about
 436 3% of the total energy consumptions and about 8% of the mechanical power consumptions.
 437 For the anti-sublimation process, all the energy requirements are concentrated in the cooling duty
 438 demand, whereas for the MEA scrubbing process more than half of the total energy consumption is
 439 related to the heat required for solvent regeneration.
 440 In Table 4, the distribution of the energy consumptions per type of operation is shown for each
 441 studied process solution. The distribution is expressed in terms of percentages of the total energy
 442 demand.

443
 444 **Table 4.** Distribution of the energy consumptions per type of operation.

| Process | Biogas compression [%] | Biogas upgrading [%] | CO₂ pressurization [%] | Biomethane liquefaction [%] |
|--|-----------------------------------|---------------------------------|--|--|
| Ryan-Holmes | 33.41 | 39.74 | 0.12 | 26.74 |
| Dual pressure low-temperature distillation | 38.19 | 31.93 | 0.00 | 29.88 |
| Anti-sublimation | 0.00 | 73.99 | 0.16 | 25.85 |
| MEA scrubbing | 0.00 | 57.40 | 7.78 | 34.82 |

445
 446 Considering this second analysis, it is possible to notice that for low-temperature processes the
 447 contribution of the CO₂ pressurization is mostly negligible, since it is carried out by means of
 448 pumps due to the availability of carbon dioxide in liquid phase. The contribution of biomethane
 449 liquefaction to the total energy requirements is similar for each considered process configuration: it
 450 lies between 25 and 30%. For biogas compression the results are analogous to the ones reported in

451 Table 3 for the mechanical power consumptions. The biggest difference among the three low-
452 temperature processes is given by the biogas upgrading step: anti-sublimation has the highest power
453 consumption since CO₂ is frosted in a single unit operation that entirely uses a single cold utility at
454 constant temperature, while the two distillation processes involve half of the energy requirements of
455 the anti-sublimation. Considering only the two distillation-based processes, the energy required by
456 the dual pressure low-temperature process is 10% less than that involved in the Ryan-Holmes
457 process since no heat duties at high temperatures are required.

458 If the amine scrubbing process is taken into account, the results summarized in Table 4 suggest that
459 the energy required for upgrading the raw biogas stream is higher in comparison with that related to
460 the two less energy-demanding low-temperature processes (*i.e.*, the dual pressure low-temperature
461 distillation process and the Ryan-Holmes process) due to the duty to be supplied to the reboiler of
462 the *Regenerative distillation* column for solvent regeneration. The biomethane liquefaction step has
463 a share of the total energy consumption which does not significantly differ from the ones of the
464 same type of operation performed in low-temperature processes. On the contrary, the CO₂
465 pressurization step contributes to the total energy consumption to a larger extent than in low-
466 temperature processes due to the inter-refrigerated multistage compression train that is necessary to
467 bring the atmospheric CO₂ gaseous stream coming from the top of the *Regenerative distillation* unit
468 to the desired pressure of 50 bar.

469 Considering the results obtained in this study in terms of energy performances, there is a good
470 margin between the low-temperature processes and the MEA scrubbing process, especially for the
471 Ryan-Holmes and the dual pressure low-temperature distillation processes (*i.e.*, for the upgrading
472 processes based on low-temperature distillation), which exploit the synergy between the
473 temperature levels at which the upgrading and the liquefaction processes are operated.

474

475 **5. Conclusions**

476 Liquid biomethane is a promising biofuel that can be obtained from upgrading and liquefaction of
477 biogas. In this work, its production has been studied considering different technologies for biogas
478 upgrading, namely three low-temperature purification technologies (*i.e.*, the Ryan-Holmes
479 extractive distillation process, a recently developed dual pressure low-temperature distillation
480 process and the anti-sublimation process) and the conventional amine scrubbing process, by means
481 of a MEA aqueous solution. These processes have been compared in terms of energy consumptions
482 evaluated by means of the net equivalent methane approach, which consists in determining the
483 amount of biomethane that is consumed within each process to supply the required thermal and
484 mechanical duties. The results of the comparison (presented in terms of the percentage of the

485 produced biomethane required by each process for LBM production) have suggested that low-
486 temperature processes require a lower amount of the produced biomethane to be used for supplying
487 energy to the process with respect to the conventional amine scrubbing process. In particular, the
488 two processes based on distillation have turned out to be the least energy-intensive ones.

489 Moreover, the comparison has been also made by considering the contributions to the global energy
490 requirements distinguished by type of energy (*i.e.*, mechanical, cooling and heating) and by type of
491 operation (*i.e.*, biogas compression, biogas upgrading, CO₂ pressurization - considered in this work
492 to obtain it in liquid phase under pressure, suitable conditions for further uses - and biomethane
493 liquefaction). The dual pressure low-temperature process requires the highest mechanical power as
494 a result of the operating pressure of the high-pressure section but, if compared with the Ryan-
495 Holmes process (also based on distillation), it does not require any heat supply. This becomes
496 crucial in the MEA scrubbing process, for which more than half of the energy consumed is related
497 to the heat required for solvent regeneration. On the contrary, the cooling duty demand at low-
498 temperature is the main source of energy consumption for the anti-sublimation process. Considering
499 the distribution of the energy consumption per type of operation, results have suggested that the
500 three low-temperature processes require very little energy for CO₂ pressurization and almost the
501 same percentage of the total energy to be consumed for biomethane liquefaction. The biggest
502 difference between them is given by the biogas upgrading step, since the anti-sublimation process
503 requires almost a twofold amount of energy for that, due to the way CO₂ is frosted within this
504 process (*i.e.*, by using a single cold utility at constant temperature). The amine scrubbing process
505 differs from the low-temperature ones because of the higher energy required for biogas upgrading
506 (due to the heat needed for solvent regeneration) and for CO₂ pressurization.

507 In conclusion, the performed analysis suggests that low-temperature processes, and the dual
508 pressure low-temperature distillation process in particular, have better performances than the
509 conventional amine scrubbing process, being the low temperatures reached in the upgrading step
510 synergistic with the production of liquid biomethane.

511

512 **References**

513 [1] L.A. Pellegrini, G. De Guido, S. Consonni, G. Bortoluzzi, M. Gatti, From biogas to biomethane:
514 How the biogas source influences the purification costs, Chem. Eng. Trans. 43 (2015) 409-414.

515 [2] EurObserv'ER, Biogas Barometer. [http://energies-renouvelables.org/observ-
516 er/stat_baro/observ/baro224_Biogas_en.pdf](http://energies-renouvelables.org/observ-er/stat_baro/observ/baro224_Biogas_en.pdf), 2014 (accessed 17.02.17).

517 [3] O. Jönsson, E. Polman, J. Jensen, R. Eklund, H. Schyl, S. Ivarsson, Sustainable gas enters the
518 European gas distribution system. Danish gas technology center, 2003.

- 519 [4] M. Persson, O. Jönsson, A. Wellinger, Biogas upgrading to vehicle fuel standards and grid
520 injection, IEA Bioenergy task, 2006.
- 521 [5] G. Soreanu, M. Beland, P. Falletta, K. Edmonson, L. Svoboda, M. Al-Jamal, P. Seto,
522 Approaches concerning siloxane removal from biogas—a review, *Can. Biosyst. Eng.* 53 (2011) 8.1-
523 8.18.
- 524 [6] L.B. Allegue, J. Hinge, K. Allé, Biogas and bio-syngas upgrading, Danish Technological
525 Institute, Aarhus (2012).
- 526 [7] S. Rasi, Biogas composition and upgrading to biomethane, University of Jyväskylä, 2009.
- 527 [8] D. Andriani, A. Wresta, T.D. Atmaja, A. Saepudin, A review on optimization production and
528 upgrading biogas through CO₂ removal using various techniques, *Appl. Biochem. Biotechnol.* 172
529 (2014) 1909-1928.
- 530 [9] D. Thrän, T. Persson, J. Daniel-Gromke, J. Ponikta, M. Seiffert, J. Baldwin, Biomethane—status
531 and factors affecting market development and trade. IEA Task 40 and Task 37 Joint Study,
532 International Energy Agency, 2014.
- 533 [10] S. Gamba, L. Pellegrini, Biogas upgrading: Analysis and comparison between water and
534 chemical scrubbing, *Chem. Eng. Trans.* 32 (2013) 1273-1278.
- 535 [11] G. Bortoluzzi, M. Gatti, A. Sogni, S. Consonni, Biomethane Production from Agricultural
536 Resources in the Italian Scenario: Techno-Economic Analysis of Water Wash, *Chem. Eng. Trans.*
537 37 (2014) 259-264.
- 538 [12] H. Cherif, C. Coquelet, P. Stringari, D. Clodic, L. Pellegrini, S. Moioli, S. Langè, Experimental
539 and Simulation Results for the Removal of H₂S from Biogas by Means of Sodium Hydroxide in
540 Structured Packed Columns, ICBST 2016: 18th International Conference on Biogas Science and
541 Technology, 2016.
- 542 [13] B. Kelley, J. Valencia, P. Northrop, C. Mart, Controlled Freeze Zone™ for developing sour gas
543 reserves, *Energy Proced.* 4 (2011) 824-829.
- 544 [14] A.S. Holmes, J.M. Ryan, Cryogenic distillative separation of acid gases from methane, Google
545 Patents, 1982.
- 546 [15] A.S. Holmes, J.M. Ryan, Distillative separation of carbon dioxide from light hydrocarbons,
547 Google Patents, 1982.
- 548 [16] L.A. Pellegrini, Process for the removal of CO₂ from acid gas, Google Patents, 2014.
- 549 [17] D. Clodic, R. El Hitti, M. Younes, A. Bill, F. Casier, CO₂ capture by anti-sublimation. Thermo-
550 economic process evaluation, 4th Annual Conference on Carbon Capture and Sequestration,
551 National Energy Technology Laboratory Alexandria (VA), USA, Alexandria, VA, USA, 2005, pp.
552 2-5.

- 553 [18] GPSA Engineering Databook, 12th ed., Gas Processors Suppliers Association (GPSA), Tulsa,
554 OK, USA, 2004.
- 555 [19] AspenTech, Aspen Hysys[®], AspenTech, Burlington, MA, 2012.
- 556 [20] G. Soave, Equilibrium constants from a modified Redlich-Kwong equation of state, Chem.
557 Eng. Sci. 27 (1972) 1197-1203.
- 558 [21] A. Holmes, B. Price, J. Ryan, R. Styring, Pilot tests prove out cryogenic acid-gas/hydrocarbon
559 separation processes, Oil Gas J. 81 (1983) 85-86.
- 560 [22] K. Kaupert, L. Hays, S. Gandhi, C. Kaehler, Flashing liquid expanders for LNG liquefaction
561 trains, 2013.
- 562 [23] M. Baccanelli, S. Langé, M.V. Rocco, L.A. Pellegrini, E. Colombo, Low temperature
563 techniques for natural gas purification and LNG production: An energy and exergy analysis, Appl.
564 Energ. 180 (2016) 546-559.
- 565 [24] A. Martin, C. Peters, New thermodynamic model of equilibrium states of gas hydrates
566 considering lattice distortion, J. Phys. Chem. C 113 (2009) 422-430.
- 567 [25] D. Clodic, M. Younes, A new method for CO₂ capture: frosting CO₂ at atmospheric pressure,
568 Sixth International Conference on Greenhouse Gas control Technologies GHGT6, Kyoto, Japan,
569 2002, pp. 155-160.
- 570 [26] CryoPur, <http://www.cryopur.com>, (accessed 15.12.16).
- 571 [27] A.L. Kohl, R. Nielsen, Gas Purification, Gulf Publishing Company, Houston, TX, USA, 1997.
- 572 [28] S. Langé, L.A. Pellegrini, P. Vergani, M. Lo Savio, Energy and economic analysis of a new
573 low-temperature distillation process for the upgrading of high-CO₂ content natural gas streams, Ind.
574 Eng. Chem. Res. 54 (2015) 9770-9782.
- 575 [29] R.N. Maddox, Gas and liquid sweetening, JM Campbell for Campbell Petroleum series, 1974.
- 576 [30] ThermExcel, http://www.thermexcel.com/english/tables/vap_eau.htm, (accessed 17.02.17).
- 577 [31] M. Kanoğlu, Exergy analysis of multistage cascade refrigeration cycle used for natural gas
578 liquefaction, Int. J. Energ. Res. 26 (2002) 763-774.
- 579 [32] W. Lim, K. Choi, I. Moon, Current status and perspectives of liquefied natural gas (LNG) plant
580 design, Ind. Eng. Chem. Res. 52 (2013) 3065-3088.
- 581 [33] Y.A. Cengel, M.A. Boles, Thermodynamics: an engineering approach, Sea 1000 (2002) 8862.
- 582 [34] R.H. Perry, D.W. Green, Perry's chemical engineers' handbook, 7th ed., New York: McGraw-
583 Hill, 2008.
- 584 [35] R. Kehlhofer, F. Hanneman, F. Stirnimann, B. Rukes, Combined-Cycle Gas and Steam Turbine
585 Power Plants, Pennwell Corp, 2009.
- 586 [36] CleaverBrooks, <http://www.cleaver-brooks.com/Reference-Center/Insights/Boiler-Efficiency->

587 [Guide.aspx](#), (accessed 17.02.17).

588 [37]

Unige,

589 http://www.ditec.unige.it/users/administrator/documents/FT2_DITEC_GG_PARTE1.pdf, (accessed
590 17.02.17).

591

592

Table 1. Values of the parameters used to calculate the biomethane equivalent to process energy streams.

| Parameter | Parameter Value | Reference |
|------------------------|-----------------|-----------|
| LHV_{CH_4} [MJ/kg] | 50 | [34] |
| η_{CC} [-] | 0.55 | [35] |
| η_B [-] | 0.8 | [36] |
| η_{II} [-] | 0.6 | [37] |
| COP_f (@ -165°C) [-] | 0.34 | This Work |
| COP_f (@ -100°C) [-] | 0.83 | This Work |
| COP_f (@ -35°C) [-] | 2.38 | This Work |
| COP_f (@ -10°C) [-] | 4.51 | This Work |

Table 2. Percentages of the total produced biomethane required by the different investigated processes for LBG production.

| Process | % LBM |
|--|---------|
| Ryan-Holmes | 15.70 |
| Dual pressure low-temperature distillation | 14.00 |
| Anti-sublimation | 21.79 |
| MEA scrubbing | 29.00 |

Table 3. Distribution of the energy consumptions by quality.

| Process | Mechanical power consumption [%] | Cooling duties consumption [%] | Heating duties consumption [%] |
|--|----------------------------------|--------------------------------|--------------------------------|
| Ryan-Holmes | 33.55 | 54.37 | 12.07 |
| Dual pressure low-temperature distillation | 38.77 | 61.23 | 0.00 |
| Anti-sublimation | 0.16 | 99.84 | 0.00 |
| MEA scrubbing | 7.78 | 34.82 | 57.40 |

Table 4. Distribution of the energy consumptions per type of operation.

| Process | Biogas compression [%] | Biogas upgrading [%] | CO₂ pressurization [%] | Biomethane liquefaction [%] |
|--|-----------------------------------|---------------------------------|--|--|
| Ryan-Holmes | 33.41 | 39.74 | 0.12 | 26.74 |
| Dual pressure low-temperature distillation | 38.19 | 31.93 | 0.00 | 29.88 |
| Anti-sublimation | 0.00 | 73.99 | 0.16 | 25.85 |
| MEA scrubbing | 0.00 | 57.40 | 7.78 | 34.82 |

Fig. 1. Process Flow Diagram of the Ryan-Holmes process.

Fig. 2. Process Flow Diagram of the dual pressure low-temperature distillation process.

Fig. 3. Process Flow Diagram of the anti-sublimation process.

Fig. 4. Process Flow Diagram of the MEA scrubbing process.

Figure 1

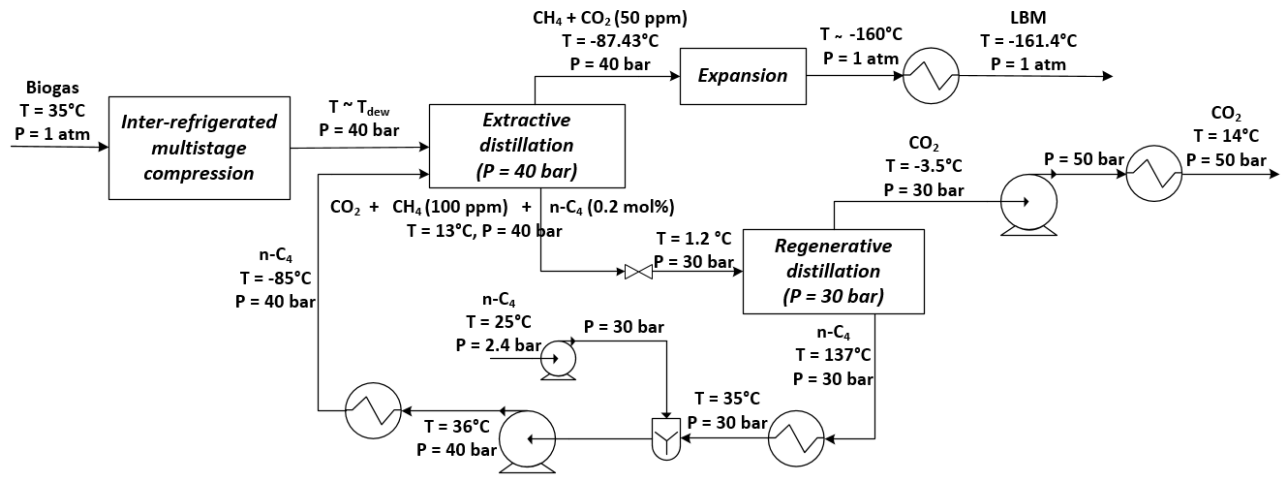


Fig. 1. Process Flow Diagram of the Ryan-Holmes process.

Figure 2

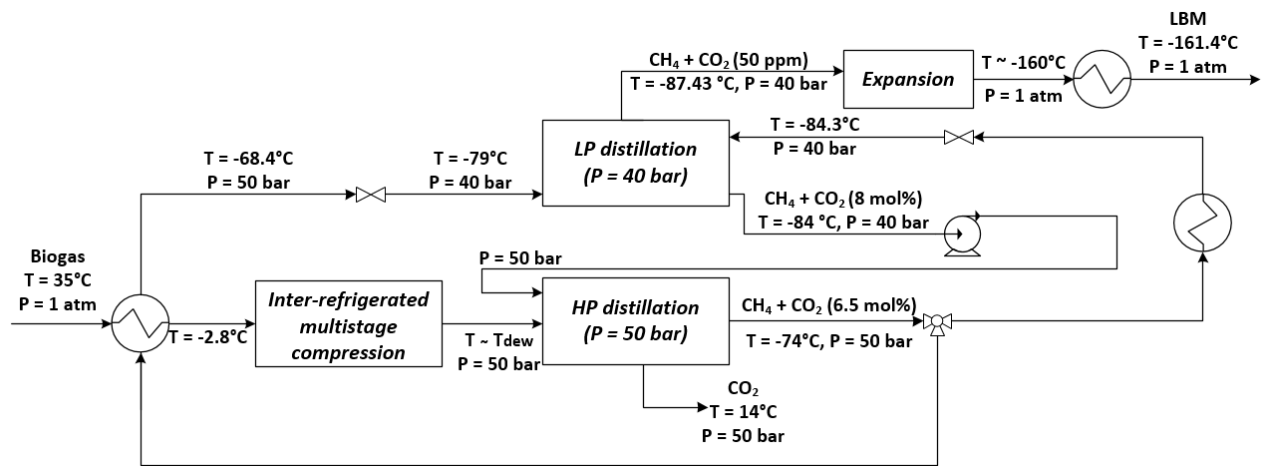


Fig. 2. Process Flow Diagram of the dual pressure low-temperature distillation process.

Figure 3

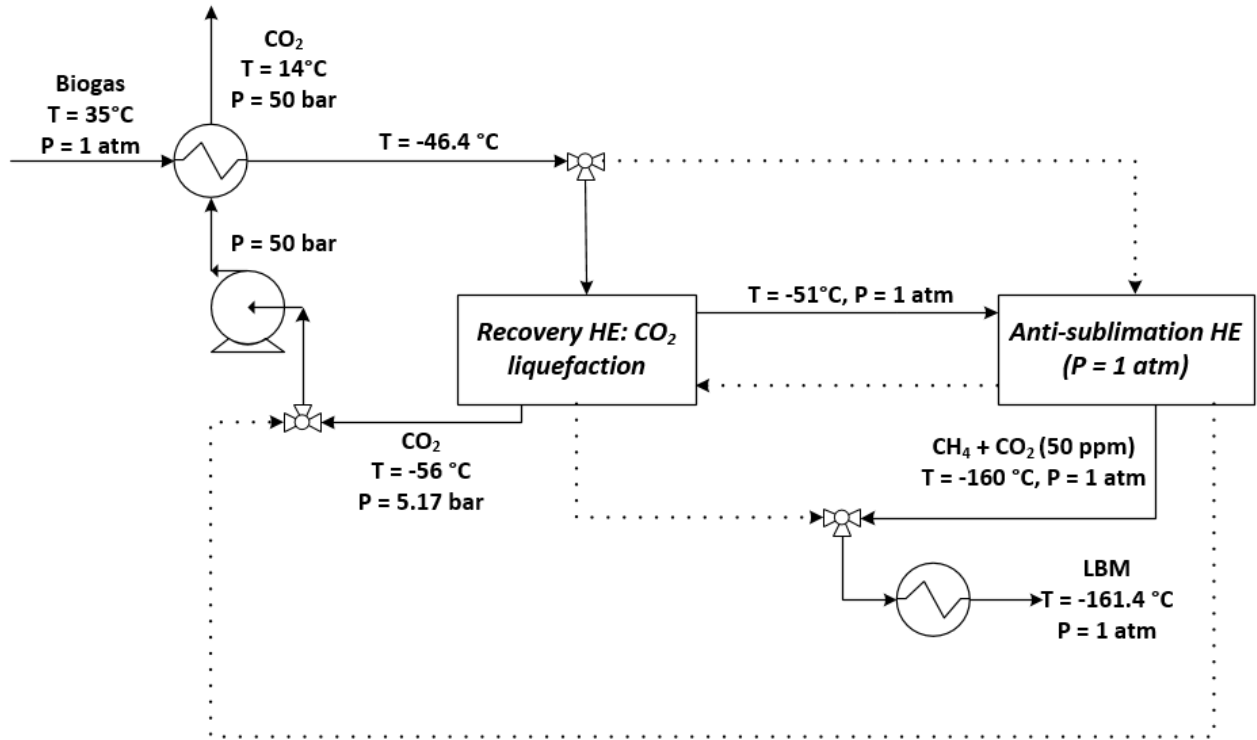


Fig. 3. Process Flow Diagram of the anti-sublimation process.

Figure 4

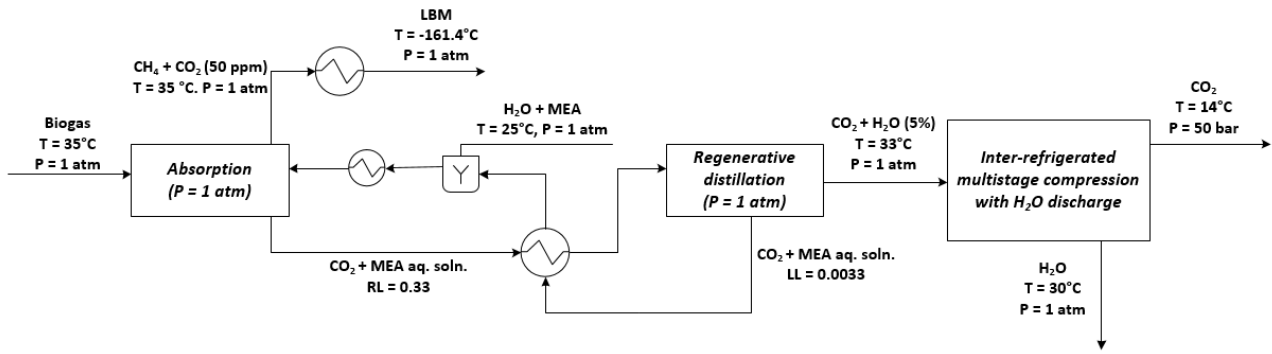


Fig. 4. Process Flow Diagram of the MEA scrubbing process.